# COMPARATIVE ANALYSIS OF PRISMA HYPERSPECTRAL AND SENTINEL-2 MULTISPECTRAL IMAGES FOR CHLOROPHYLL-A AND TURBIDITY MAPPING OF TAAL LAKE

A. M. Hernando [1]*, A. M. Piano [1], A. C. Blanco [1,2,4], J. M. Medina [1,2], A. Y. Manuel [3]

[1] Department of Geodetic Engineering, University of the Philippines Diliman, Quezon City, Philippines - (aphernando, appiano1, acblanco, jmmedina)@up.edu.ph

[2] Training Center for Applied Geodesy and Photogrammetry, University of the Philippines Diliman, Quezon City, Philippines

[3] Centre for Remote Imaging, Sensing, and Processing, National University of Singapore, Singapore 119076 - aymanuel@nus.edu.sg

[4] Philippine Space Agency, Quezon City, Philippines - ariel.blanco@philsa.gov.ph

**KEY WORDS:** Remote Sensing**,** Water quality, Water Colour Simulator (WASI), NDCI, NDTI

**ABSTRACT:**

Freshwater bodies like Taal Lake play a pivotal role in providing essential resources like fresh drinking water and in supporting local livelihoods. This study aimed to examine the environmental conditions of Taal Lake by quantifying chlorophyll-a (chl-a) and turbidity levels with Water Colour Simulator (WASI) and water quality indices, specifically with Sentinel-2 and PRISMA imagery. The results from the satellite image-derived data revealed discernible variations in chlorophyll-a and turbidity concentrations across different regions of Taal Lake. Higher chlorophyll-a was consistently observed in the western regions (1.3-5.9 μg/L for Sentinel-2; 1.4-5.4 μg/L for PRISMA), while lower concentrations were found in the south (1.7-3.4 μg/L for Sentinel-2; 1.9-3.3 μg/L for PRISMA). Meanwhile, turbidity values were higher in the eastern and northeastern parts (0.15-0.59 mg/L for Sentinel-2; 0.13-0.51 mg/L for PRISMA). Water quality indices (NDTI & NDCI) also supported these findings. The findings of this comparative analysis between PRISMA hyperspectral and Sentinel-2 multispectral imagery demonstrate the potential of both satellite systems in providing valuable insights into the spatial distribution of water quality parameters in Taal Lake. Nonetheless, discrepancies observed in the scatter plots and inversion failures in PRISMA underscore the need for further research and refinement in utilizing PRISMA data with the WASI model. This study highlights the significance of freshwater bodies and the importance of monitoring their health for the well-being of communities and the environment.

## 1. INTRODUCTION

Freshwater is essential for communities worldwide, serving as a source of clean drinking water (Davis, 2012). However, contamination of surface waters and sewage from urban development (Bhateria & Jane, 2016) raise global concerns. The Philippines, in particular, has implemented strict regulations to conserve sources of freshwater such as wetlands and lakes (Vasistha & Ganguly, 2020; DENR-EMB, 2018).

The Unified Rules and Regulations for Fisheries (URRF), for one, exemplify these efforts. Managed by the Taal Volcano Protected Landscape - Protected Areas Management Board (TVPL-PAMB), URRF supervises the maintenance of Taal Lake in Batangas (Martinez & Galera, 2011). Despite these efforts, illegal fish cage operations persist, harming fish populations and causing algae blooms (Luistro, 2008). The 2020 eruption of Taal Volcano (Del Castillo et al., 2020) poses further water quality concerns due to ashfall and potential magmatic releases.

Continuously monitoring these bodies of water is essential to comprehending and mitigating the various factors that affect their health and sustainability. Parameters used to characterize water quality encompass a spectrum of physical, chemical, and biological attributes, including color, temperature, taste, turbidity, pH, chlorophyll, bacteria, and algae (Department of Water and Environmental Regulation, n.d.; Sensorex, 2021). Chlorophyll-a and turbidity, which includes inorganic and organic suspended matter, exert a significant influence on the inherent optical characteristics of water bodies, particularly inland ones (Ma et al., 2007). If more progress is to be achieved in the extraction of other constituent concentrations from colored images of sediment-dominated waters, it is essential that the estimates of suspended material concentrations be made with greater accuracy (Binding et al., 2005).

Traditionally, the assessment of the properties of lake water relied on methods such as hazard quotients and water quality indices (Bhateria & Jane, 2016). However, the rapid evolution of modern technology has ushered in a new era in water quality monitoring with remote sensing techniques particularly hyperspectral and multispectral imaging. These cutting-edge techniques have transcended the limitations of traditional in-situ methods (Zhang et al., 2020).

Hyperspectral and multispectral imagery provide spectral data to estimate chlorophyll, suspended particulate matter (SPM), and turbidity via spectral indices (Bansod et al., 2018). Hyperspectral data, with high spectral resolution, enhances surface material detection and chemical and biological analysis (Adam et al., 2010 as cited in Mbuh, 2019). Hyperspectral data also aids in recognizing chlorophyll and algae in various aquatic environments (Niroumand-Jadidi et al., 2020). However, the comparative performance of hyperspectral and multispectral imaging in retrieving optically active constituents remains underexplored, leaving a gap in our understanding of their relative effectiveness.

Our research aims to fill this gap by comparing hyperspectral imagery from PRISMA with multispectral imagery from Sentinel-2 to estimate chlorophyll-a and turbidity in Taal Lake,

---

* Corresponding author

Batangas. Utilizing advanced water quality indices and the Water Colour Simulator (WASI) processing software, we seek to comprehensively understand water quality dynamics in this study area.

## 2. METHODOLOGY

A comparative analysis was performed to assess the relationship of chlorophyll-a and turbidity with in-situ, multispectral, and hyperspectral data. The implications and the relevance of satellite imagery in mapping the selected water quality parameters in Taal Lake, Batangas were also examined. Figure 1 presents the general workflow that was implemented in the study.

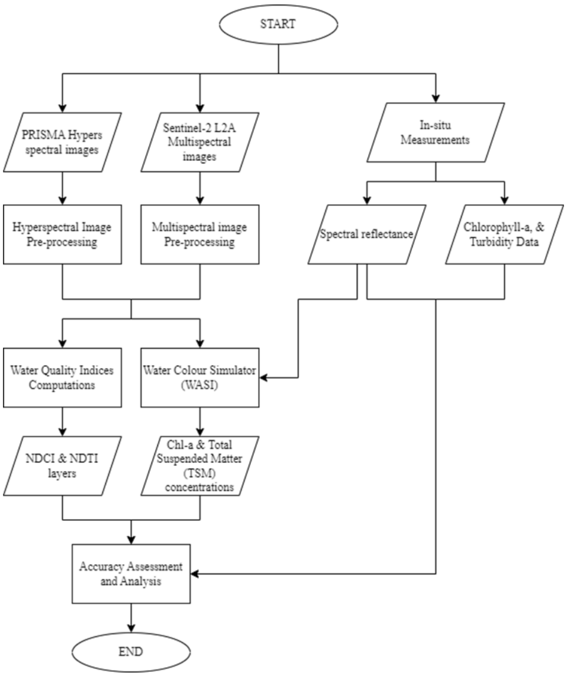

**Figure 1.** General Workflow of the Study

### 2.1 Study Area

Taal Lake (Figure 2) is a freshwater body situated within a complex volcanic caldera in Batangas, Philippines. It has an average depth of 90.8 m (maximum: 198 m) and a surface area of 234.2 km$^2$ (Perez et al., 2008; Taal Volcano, nd). The lake has 37 tributaries, and its single outflow is the Pansipit River, which flows into Balayan Bay (Britannica, 2020).

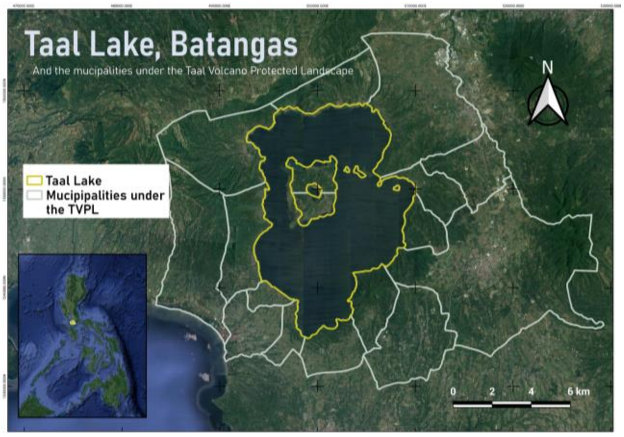

**Figure 2.** Map of Taal Lake, Batangas

Taal Lake falls under the protection of the Taal Volcano Protected Landscape (TVPL) as a National Park, governed by the NIPAS Act (RA 7586) and Presidential Proclamation 923. Classified as Class C water under DENR Administrative No. 2016-08 and 2021-19, it serves multiple purposes, including fish propagation, recreation, and agricultural use. This lake is a vital resource for nearby communities, supporting their livelihoods through fish farming and supplying freshwater to areas like Tagaytay, Cavite, while also drawing tourists to its scenic beauty (White et al., 2016; Pabico et al., 2015).

However, some concerns arise about Taal Lake's environmental health. Medallion & Garcia (2021) found elevated chemical properties due to waste disposal and fish farm fertilizers, impacting the ecosystem. Additionally, White et al.'s 2016 report noted overcapacity in aquaculture structures, leading to high chlorophyll-a and SPM levels, low dissolved oxygen, and reduced animal presence in some areas. Protecting Taal Lake's aquatic resources is crucial for its sustainability, necessitating proactive measures.

### 2.2 Data Acquisition

**2.2.1 Acquisition of Satellite Images**: The hyperspectral satellite image of Taal Lake was acquired from PRISMA and the multispectral satellite image was acquired from Sentinel-2. The only available PRISMA and Sentinel-2 images closest to the field survey date, with the least cloud cover were taken on April 08, 2023, and April 02, 2023, respectively, which are approximately three weeks from the field data acquisition date. The PRISMA image, which contains VNIR and SWIR data cubes, was requested and downloaded from PRISMA's data search and download portal, 'https://prisma.asi.it/'. On the other hand, the Sentinel-2 L2A image was downloaded from Copernicus Open Access Hub.

**2.2.2 Field Data Collection:** An on-site field survey was conducted in Taal Lake, Batangas on March 12, 2023, to acquire in-situ spectral reflectance data, chlorophyll-a, and turbidity. The instruments that were used to measure these parameters are: spectrometer, and turbidity and chlorophyll logger, respectively. The data gathered during this fieldwork were not used to validate the results of the image processing due to temporal discrepancies, but as a reference for the spatial variability of the water quality parameters of the lake.

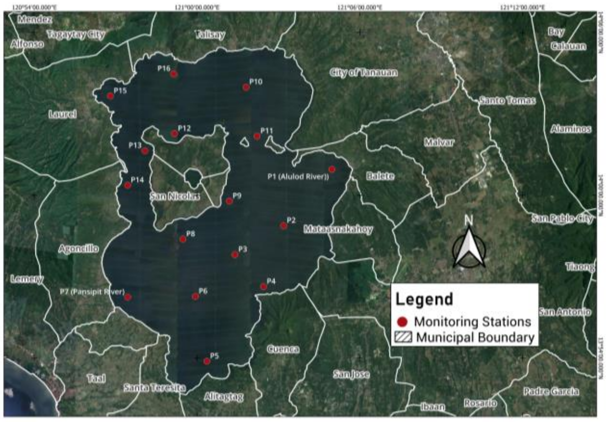

**Figure 3.** Taal Lake Field Monitoring Stations

A total of 16 stations were established throughout the study area to measure water quality parameters. Figure 3 shows the map

https://doi.org/10.5194/isprs-archives-XLVIII-4-W8-2023-293-2024

showing the established monitoring stations for the purpose of this study.

## 2.3 Pre-Processing of Data

**2.3.1 Satellite Image Pre-processing:** The PRISMA L2D data in HDF5 format was converted into ENVI format, where noise and unnecessary spectral bands were filtered using forward and inverse Minimum Noise Fraction (MNF) Estimate Noise Statistics. A spectral indices-based cloud detection technique, using the Cloud Index (*Equation 3 & 4*) developed by Zhai et al. (2018), was implemented to filter clouds in the PRISMA image.

$$Cloud\ Index = CI_2 = \frac{B_B + B_G + B_R + B_{NIR}}{4} \tag{3}$$

$$CI_2 > T_2 \tag{4}$$

where $B_B$, $B_G$, and $B_R$ represent the blue, green, and red bands in the visible range, respectively, while the $B_{NIR}$ represents the NIR band. To isolate the clouds further, *Equation 4* was then used. $CI_1$ is the 2nd formula for the Cloud Index (*Equation 3*) and $T_2$ is a large threshold value denoting a relatively larger value as clouds are generally brighter and have a higher reflectance than land materials.

For the Sentinel-2 image, cloud masking and deglinting procedure of Hedley, et al. (2004) and Martin, et al. (2016), respectively, were performed using SNAP to eliminate sea surface-level effects such as bright white 'sea glints' from high-resolution satellite images such as Sentinel and Planet. The Deglint Processor tool eliminated sun glints, and the LandCloudWhiteCapMask Processor detected and removed hovering clouds.

Both pre-processing methods resulted in clear and refined images for further analysis.

**2.3.2 In-situ Data:** The spectral reflectance data were processed, including noise elimination, outlier removal, and smoothening using the Savitzky-Golay filter (Niedźwiecki, et al., 2021; Guest, 2012). These steps ensured a clear and precise representation of the data, crucial for subsequent analysis.

Simultaneously, in-situ water quality parameters, such as chlorophyll-a and turbidity, were inspected to identify outliers. The data was summarized for each field station, and the mean of the obtained chlorophyll-a and turbidity values were calculated for correlation analysis.

## 2.4 Data Processing and Analysis

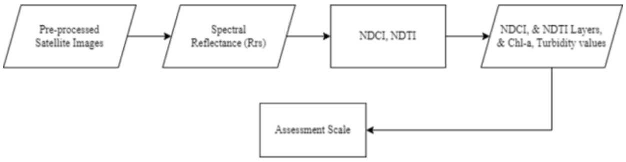

**Figure 4.** Water Quality Index Processes

**2.4.1 Water Quality Indices (WQI)**: Van Nguyen et al. (2020)'s study on estimating water quality used spectral reflectance from MERIS images as input as well as their corresponding in-situ measurements for chl-a retrieval model determination. This study mirrored this method with the Normalized Difference Chlorophyll Index (NDCI) and Normalized Difference Turbidity Index (NDTI). Figure 4 shows the workflow for the water quality indices.

Selecting the right spectral bands is critical for water quality assessments, especially when dealing with hyperspectral data, which has finer bandwidths. These bands offer specific information about the water's optical properties and are key to deriving parameters like chlorophyll-a concentration, turbidity, and suspended matter. In this study, bands for calculating water quality indices in hyperspectral images were chosen based on the most sensitive region in the corresponding multispectral band's spectral response function.

$$NDCI = \frac{Red\ Edge\ 1 - Red}{Red\ Edge\ 1 + Red} \tag{5}$$

To calculate NDCI (*Equation 5*), Mishra (2012)'s methodology was used, utilizing reflectance values at 665 nm and 708 nm. Band 37 (703.74 nm) in the hyperspectral image is closer to the most sensitive portion of the spectral response function of Sentinel-2 Band 5, making it the preferred choice. Figure 6 shows the spectral response function of the bands used for the calculation of NDCI.

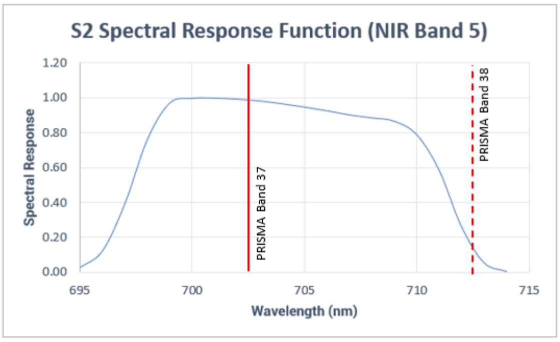

**Figure 5.** Spectral Response function of the Sentinel-2 Band 5 (NIR) with candidate PRISMA bands

Meanwhile, PRISMA Bands 21 (559.02 nm) and 32 (655.42 nm), were chosen in lieu of Sentinel-2 Band 3 (green) and Band 4 (red), respectively. These bands were chosen based on the wavelength where the particular band is the most sensitive. Figure 6 shows the spectral response function for the Sentinel-2 green and red bands which are needed to calculate for NDTI (*Equation 6*).

$$NDTI = \frac{Red - Green}{Red + Green} \tag{6}$$

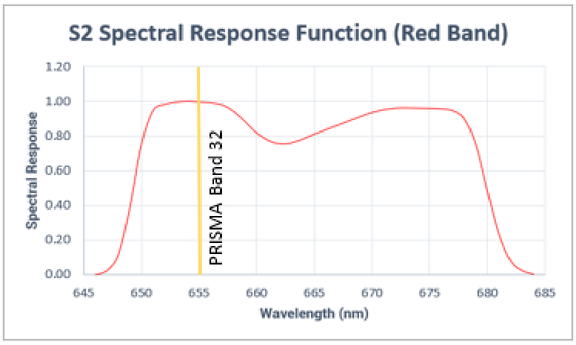

**Figure 6.** Spectral Response function of the Sentinel-2 Red Band with the chosen PRISMA band

This contribution has been peer-reviewed.
https://doi.org/10.5194/isprs-archives-XLVIII-4-W8-2023-293-2024 | © Author(s) 2024. CC BY 4.0 License.

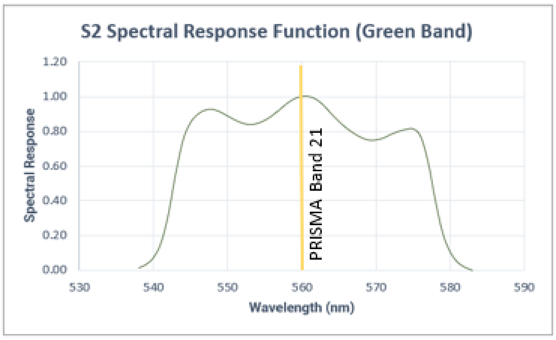

**Figure 7.** Spectral Response function of the Sentinel-2 Green Band with the chosen PRISMA band

To provide a more comprehensive qualitative assessment, the study also adapted assessment scales for the generated measurements from the indices. In general, NDTI values range from -0.2 to greater than +0.25 such that a lower value indicates clear water while a higher value indicates high turbidity (Sharma et al., 2014). Bid and Siddique (2019)'s study classified NDTI images to low, medium, and high turbidity levels based on the mean and standard deviation computed with the help of GIS software. This study utilized and modified this method in assessing the turbidity levels. These three levels were based on the formula for standard criterion in categorizing turbidity levels (Somvanshi et al., 2011).

Table 1 shows the scale used to assess turbidity measurements from NDTI values as based on Bid and Siddique (2019)'s principle of different turbidity values:

| Range of Turbidity | Formula | Value for Sentinel-2 (mg/L) | Value for PRISMA (mg/L) |
|---|---|---|---|
| **Low** | $< x - \sigma$ | < -0.209 | < -0.254 |
| **Medium** | $x - \sigma$ to $x + \sigma$ | -0.209 – 0.745 | -0.254 – 0.038 |
| **High** | $> x + \sigma$ | > 0.745 | > 0.038 |

**Table 1.** Derived assessment scale (Bid & Siddique, 2019)

**2.4.2 Water Colour Simulator (WASI)**: Water Colour Simulator (WASI) was used in processing hyperspectral PRISMA and multispectral Sentinel-2 Level-2A products to derive estimates of water quality parameters. According to Gege (2014), WASI is a software tool used to simulate and analyze the most common types of spectral observations of open waterways under outdoor settings.

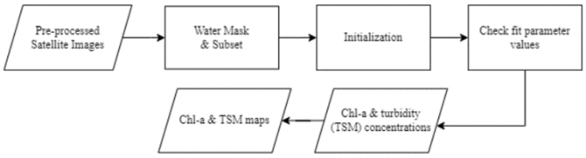

**Figure 7.** Water Colour Simulator (WASI) processes

Parameterizations of WASI employed in the processing of Taal Lake images were established using the inversion outputs derived from the field spectral measurements. These parameters serve as a crucial foundation for accurately characterizing and analyzing the optical properties of Taal Lake, enabling comprehensive and reliable assessments of its water quality, and associated environmental dynamics (Manuel, 2022).

Eight sampling points were selected for data collection and analysis. The selection process considered various factors, including the concentrations of chlorophyll-a (chl-a) and turbidity, as determined through field measurements. After spectral fitting, the values of each parameter fit used in inverting the spectra of each chosen point were then averaged.

| Points | Chlorophyll-a *C[0]* | Green Algae *C[1]* | SPM *C_X* | CDOM *C_Y* | sun glint *g_dd* |
|---|---|---|---|---|---|
| **P1** | 4.239 | 0.9204 | 0.2349 | 0 | 0.8968 |
| **P2** | 7.511 | 0.1729 | 0.3388 | 0 | 0.8288 |
| **P3** | 4.807 | 0.01047 | 0.2616 | 0 | 0.8421 |
| **P4** | 2.914 | 0.1442 | 0.4002 | 0.02352 | 0.9096 |
| **P5** | 3.935 | 0.2871 | 0.1887 | 0 | 0.8296 |
| **P6** | 3.852 | 0 | 0.1842 | 0 | 0.8296 |
| **P7** | 4.337 | 0 | 0.2788 | 0 | 0.8269 |
| **P8** | 3.669 | 0 | 0.2193 | 0 | 0.9090 |

**Table 2.** WASI fit parameters for the sample points in Sentinel-2

| Points | Chlorophyll-a *C[0]* | Green Algae *C[1]* | SPM *C_X* | CDOM *C_Y* | sun glint *g_dd* | phytoplankton backscatter *bbs_phy* |
|---|---|---|---|---|---|---|
| **P1** | | | | | | |
| **P2** | 2.425 | 0 | 0.1 | 0 | 0.0008 | 0.1586 |
| **P3** | 1.666 | 0 | 0.1 | 0 | 0 | 0.1469 |
| **P4** | 0.195 | 0.0171 | 0.1 | 0.040 | 0.1418 | 0.0010 |
| **P5** | 2.703 | 0 | 0.1 | 0 | 0.1608 | 0.0011 |
| **P6** | 3.034 | 0.2559 | 0.1 | 0 | 0.1681 | 0.0012 |
| **P7** | 2.974 | 0 | 0.2612 | 0 | 0.1238 | 0.1233 |
| **P8** | 2.066 | 0 | 0.1 | 0 | 0.1397 | 0 |

**Table 3.** WASI fit parameters for the sample points in PRISMA

Table 2 and Table 3 show the resulting fit parameters and corresponding values based on the spectral fitting done on WASI. These averaged values were used as initialization values for WASI, ensuring the incorporation of variability and enhancing the accuracy of subsequent spectral fitting analyses.

| Parameter | Initial | Min | Max |
|---|---|---|---|
| **C[0]** *Chlorophyll-a* | 4.408 | 0 | 100 |
| **C[1]** **Green Algae** | 0.1919 | 0 | 1000 |
| **C_X** *SPM (for Turbidity)* | 0.2633 | 0.100 | 1000 |
| **C_Y** *CDOM* | 0.0029 | 0 | 100 |
| **g_dd** *Sun Glint* | 0.8630 | 0 | 1 |

**Table 4.** Initialization, minimum, and maximum parameter values for running WASI for Sentinel-2

| Parameter | Initial | Min | Max |
|---|---|---|---|
| **C[0]** *Chlorophyll-a* | 2.1519 | 0 | 100 |
| **C[1]** *Green Algae* | 0.0390 | 0 | 1000 |
| **C_X** *SPM (for Turbidity)* | 0.1230 | 0 | 1000 |
| **C_Y** *CDOM* | 0.0057 | 0 | 100 |
| **Phytoplankton backscatter bbs_phy** | 0.0617 | 0 | 1 |
| **g_dd** *sun glint* | 0.1050 | 0 | 1 |

**Table 5.** Initialization, minimum, and maximum parameter values for running WASI for PRISMA

Table 4 shows the key fit parameters used for Sentinel-2. It includes chlorophyll-a, Green Algae, SPM, CDOM, and sun glint. These indicators vary within each pixel, influencing output images tailored to these parameters. Meanwhile, Table 5, for PRISMA analysis, introduces additional parameters, notably phytoplankton backscatter, due to unique sensor characteristics that will refine spectral fitting. Sun glint's incorporation in both analyses is crucial, considering its impact on overestimating parameter estimation, necessitating a comprehensive approach for precise lake ecosystem assessment using Sentinel-2 and PRISMA imagery.

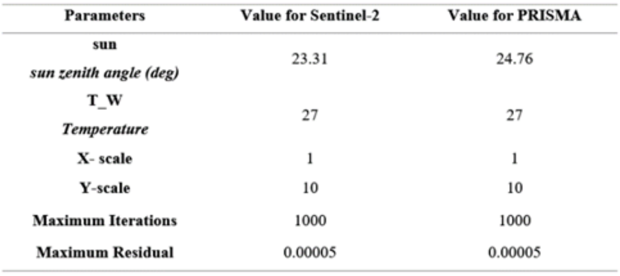

| Parameters | Value for Sentinel-2 | Value for PRISMA |
|---|---|---|
| **sun**<br>***sun zenith angle (deg)*** | 23.31 | 24.76 |
| **T_W**<br>***Temperature*** | 27 | 27 |
| **X- scale** | 1 | 1 |
| **Y-scale** | 10 | 10 |
| **Maximum Iterations** | 1000 | 1000 |
| **Maximum Residual** | 0.00005 | 0.00005 |

**Table 6.** Constant parameters

Table 6 shows the constant parameters used for both satellite images. Several parameters were established in WASI for the purpose of achieving accurate results. These parameters consider both study site's boundary conditions and fit parameters that are chosen based on the specific satellite data and the characteristics of the study area.

### 2.6 Variability and Spatial Distribution

Chlorophyll-a and turbidity data derived from the satellite images in the WASI-2D application, as well as values obtained from the water quality indices, were compared with the in-situ measurements in terms of coefficient of determination ($R^2$) and the slope of the best fit line. A higher value for $R^2$ would mean that there is a greater correlation between the two parameters obtained from the field and the values derived in the indices and in WASI. Scatter plots and correlations plots were also used to visualize the $R^2$ value and to have a further understanding of the generated values.

## 3. RESULTS AND DISCUSSION

### 3.1 Index-based Water Quality

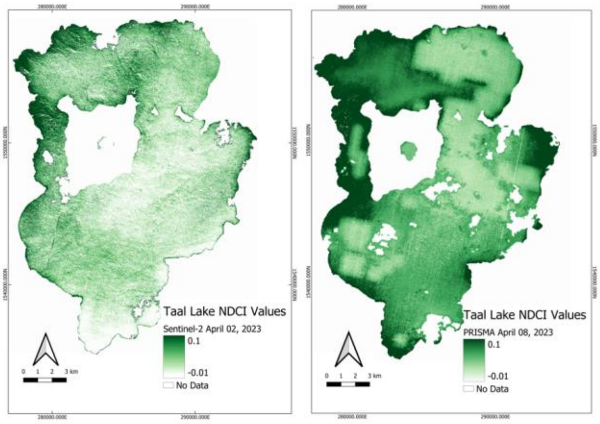

**Figure 7.** NDCI Map of Taal Lake from Sentinel 2 (left) and PRISMA (right)

Shown in Figure 7 is the NDCI map produced from Sentinel-2 and PRISMA images. In the northwestern portion of the lake, high NDCI values were observed on both images, extending to the south. The NDCI generated image of PRISMA noticeably has darker and apparent areas indicative of high index values compared to the Sentinel-2 image, especially in the northern side of the lake. This portion follows the area where sun glints are evident, which distorts the values calculated in the area. Nonetheless, other portions of the lake from both images have similar spatial distribution, with index values ranging from -0.02 to 0.04, which translates to a maximum of 25 µg/L based on Mishra's (2012) scale.

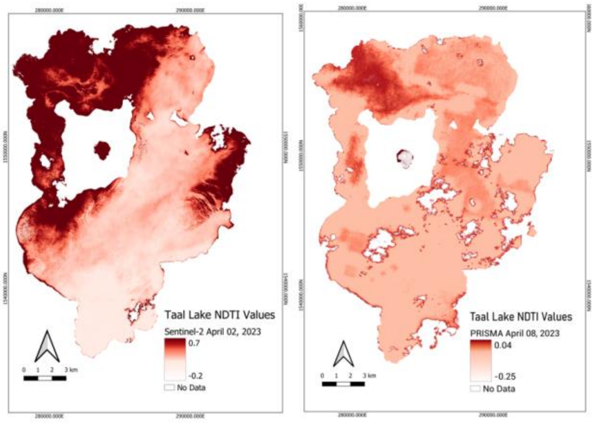

**Figure 8.** NDTI Map of Taal Lake from Sentinel 2 (left) and PRISMA (right)

Figure 8 shows the NDTI maps for Sentinel-2 and PRISMA. In the northwestern and in the middle east portion of the lake, Sentinel-2 image revealed medium to high turbidity based on index values ranging from 0.3 to 1.4. Similarly, in the northwestern and eastern regions of the lake, PRISMA data showed high turbidity, with index values ranging from 0.1 to 0.6. Low turbidity was observed in the southern and northeastern parts of the lake, with NDTI values less than -0.2 for Sentinel-2 and less than -0.25 for PRISMA.

### 3.2 WASI-2D Outputs

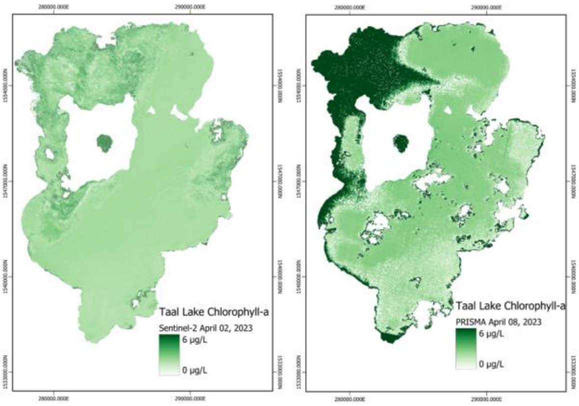

**Figure 9.** Map of Chlorophyll-a (chl-a) from Sentinel-2 (left) and PRISMA (right)

Figure 9 shows the chlorophyll-a concentration map generated by WASI 2D for both Sentinel-2 and PRISMA. The analysis of these images revealed distinct variations in chlorophyll-a concentrations across different regions of Taal Lake. In the west side of Taal Lake situated, high concentrations of chlorophyll-a ranging from 1.3 to 5.9 µg/L were observed for Sentinel-2 data. Similarly, the PRISMA-derived output exhibited chlorophyll-a concentrations ranging from 1.4 to 5.4 µg/L. Additionally, low concentrations of chlorophyll-a were also found in the southern portion of the lake for Sentinel-2 data, in which chlorophyll-a concentrations ranged from 1.7 to 3.4 µg/L. Similarly, for PRISMA data, concentrations of chlorophyll-a ranged from 1.9 to 3.3 µg/L were observed in the southern portion of the lake.

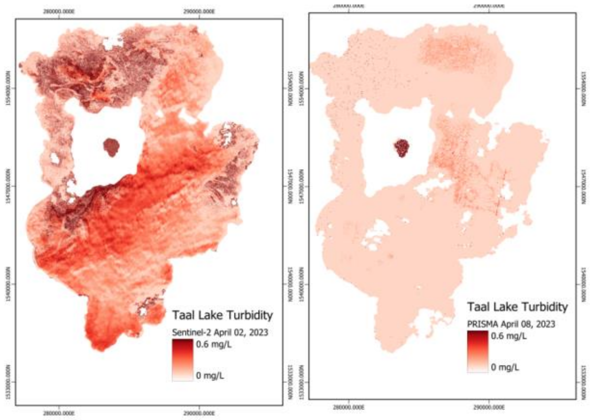

**Figure 10.** Map of Turbidity from Sentinel-2 (left) and PRISMA (right)

Figure 10 shows the estimated turbidity generated by WASI-2D for both Sentinel-2 and PRISMA. Turbidity concentrations were only observed in the eastern and northeastern portions of Taal Lake for PRISMA. In these locations, turbidity concentrations ranged from 0.15 to 0.59 mg/L for Sentinel-2, and 0.13 to 0.51 mg/L for PRISMA. The obtained turbidity values are then compared to the standards outlined in DAO-2016-08, specifically for Class C waters applicable to Taal Lake. Based on the established threshold of 80 mg/L according to DAO-2016-08, the turbidity concentrations obtained from the WASI analysis falls under the standards for Class C waters. However, it should be noted that the remaining areas of Taal Lake exhibited a turbidity concentration value of 0.1, which is the default minimum value set for turbidity in WASI. This discrepancy can be attributed to the failure of the model inversion to fit a value that is within the described parameter limits. These findings highlight the agreement of concentration values of turbidity within Taal Lake.

### 3.3 Comparative Analysis

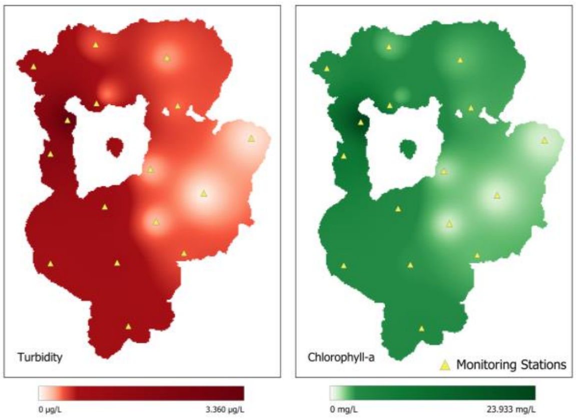

**Figure 11.** Spatial Distribution of in-situ chlorophyll-a and turbidity values using IDW Interpolation

The spatial distributions of chlorophyll-a and turbidity derived from the WASI output of Sentinel-2 and PRISMA, as well as the index-based methods, were compared to the spatial distribution of chlorophyll-a and turbidity obtained from the field, as shown in the interpolated concentrations in Figure 11. Satellite-derived maps (Sentinel-2 and PRISMA) and field data interpolation consistently show higher chlorophyll-a concentrations in the northern and western regions of Taal Lake, attributed to phytoplankton abundance due to elevated levels of nutrients and minerals near fish farms. Southern areas, with less aquaculture, exhibit lower chlorophyll-a levels. This indicates WASI effectively derived water quality parameters, matching field data's spatial patterns.

Moreover, when evaluating the spatial distribution of turbidity in Taal Lake, it is worth noting that the WASI-generated turbidity map for PRISMA exhibited a high occurrence of inversion failure, rendering it less reliable for interpretation. The inversion failure observed in the PRISMA data may be attributed to a combination of factors, including differences in spectral characteristics, resolution, and sensor calibration between PRISMA and Sentinel-2. These disparities can impact the accurate retrieval of turbidity values and hinder the generation of turbidity maps using PRISMA data.

Nonetheless, the NDTI maps from Sentinel-2 and PRISMA, along with Sentinel-2's WASI-generated data, align with field measurements. They show higher turbidity in the northwestern, northern, and eastern areas of Taal Lake, with lower concentrations in the south, confirming their ability to capture turbidity patterns. To further explain the strength and direction of the relationship of the variables, the correlation between chlorophyll-a and turbidity values from the water quality indices and WASI were calculated.

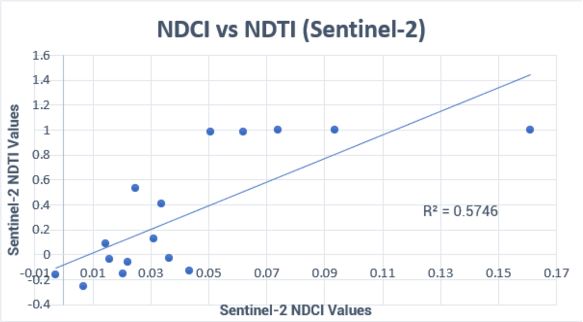

**Figure 12.** Correlation plot between the observed NDCI and NDTI values for Sentinel-2

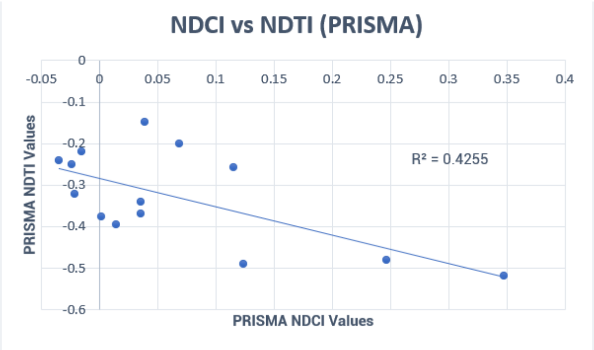

**Figure 13.** Correlation plot between the observed NDCI and NDTI values for PRISMA

Figure 12 and Figure 13 shows the relationship strength between the NDCI and NDTI values observed from Sentinel-2 and PRISMA, respectively. Sentinel-2 demonstrated a stronger positive correlation ($R^2 = 0.5746$) than PRISMA ($R^2 = 0.4318$), indicating a similar relationship to field data. PRISMA, however, displayed a negative relationship between chlorophyll-a and turbidity.

The contrasting results can be attributed to several factors, including a six-day time gap between satellite acquisitions, introducing temporal challenges that could influence water quality characteristics. Even so, validation of these claims is challenging. Additionally, PRISMA's index-generated output exhibited an inverse relationship, suggesting that inorganic or sediment-driven turbidity might limit light penetration, reducing algae production and chlorophyll concentrations (Nunes et al., 2022). These findings hint at potential algorithmic differences or interpretation limitations with hyperspectral data.

Despite PRISMA boasting a higher spectral resolution, it is constrained by its lower spatial resolution of 30 meters. In contrast, Sentinel-2 exhibits the opposite characteristic with a higher spatial resolution of 10 meters but lower spectral resolution. Consequently, both satellite systems yielded comparable results in terms of spatial distribution and general concentration values for chlorophyll-a and turbidity in Taal Lake. This remarkable similarity in outcomes can be attributed to the combined utilization of PRISMA's spectral resolution and Sentinel-2's spatial resolution. The spatial resolution of Sentinel-2, being three times better than that of PRISMA, enables it to capture finer details and surface features with greater precision. This finer spatial resolution contributes to the accurate representation of spatial distribution patterns of chlorophyll-a and turbidity in Taal Lake. On the other hand, while PRISMA's spatial resolution is lower, its superior spectral resolution allows for more detailed characterization of the optically active constituents in the water.

## 4. CONCLUSION

The comparative analysis of PRISMA and Sentinel-2 images for chlorophyll-a and turbidity mapping demonstrated the potential of both satellite systems in providing valuable insights into the spatial distribution of water quality parameters. While both systems showed similar spatial patterns for both chlorophyll-a and turbidity, the discrepancies observed in the scatter plots and inversion failures in PRISMA may be attributed to factors such as differences in sensor characteristics compared to Sentinel-2, or local events which occurred during the temporal difference between the two satellite images. This highlights the need for further research and refinement in the utilization of PRISMA data with the WASI model. In conclusion, the results demonstrate comparable outcomes between Sentinel-2 and PRISMA in mapping chlorophyll-a and turbidity in Taal Lake. Sentinel-2's advantage lies in its higher spatial resolution, providing more detailed characterization, while PRISMA offers higher spectral resolution for enhanced spectral analysis. The selection between the two satellite images depends on specific study requirements, such as spatial detail or spectral analysis.

## ACKNOWLEDGEMENTS

We give our sincere appreciation to the Mayor’s Office of Talisay, Batangas and the Talisay MDRRMO, for their cooperation, allowing us to conduct our fieldwork, and accommodating to our needs and requests and to the Batangas Inland Fisheries Technology Outreach Station under the Bureau of Fisheries and Aquatic Resources IV-A for their support and cooperation in giving us needed information crucial to our research.

Lastly, this study would not have been possible without our friends and families’ unwavering love and support, and who have given us strength to push through.

## REFERENCES

Bid, S., & Siddique, G., 2019. Identification of seasonal variation of water turbidity using NDTI method in Panchet Hill Dam, India. *In Modeling Earth Systems and Environment, Springer Science and Business Media*. Vol. 5, Issue 4, pp. 1179–1200. https://doi.org/10.1007/s40808-019-00609-8

Gege, P., 2014. WASI-2D: A software tool for regionally optimized analysis of imaging spectrometer data from deep and shallow waters. *Computers and Geosciences*, 62, 208–215. https://doi.org/10.1016/j.cageo.2013.07.022

Manuel, A., Blanco, A. C., Tamondong, A. M., Jalbuena, R., Cabrera, O., & Gege, P., 2020. Optmization of Bio-Optical Model Parameters for Turbid Lake Water Quality Estimation Using Landsat 8 and Wasi-2d. I*nternational Archives of Photogrammetry, Remote Sensing and Spatial Information Sciences - ISPRS Archives*, 42(3/W11), pp. 67–72. https://doi.org/10.5194/isprs-archives-XLII-3-W11-67-2020

Manuel, A., 2022. Parameterization of the Bio-optical Model WASI-2D for Water Quality Mapping of Laguna Lake using Sentinel-3 Imagery. *National Graduate School of Engineering, University of the Philippines Diliman*.

Martinez, F. B., & Galera, I. C., 2011. Academic Research International Monitoring And Evaluation Of The Water Quality Of Taal Lake, Talisay, Batangas, Philippines. Academic *Research International*, 1(1). www.savap.org.pk

Medallon, M. C. & Garcia, E., 2021. 11 Physical and chemical properties of water: case of Taal Lake, *Philippines. International Journal of GEOMATE*. Vol.21, Issue 83, pp. 11-19. https://doi.org/10.21660/2021.83.5658

Mishra, S., & Mishra, D. R., 2012. Normalized difference chlorophyll index: A novel model for remote estimation of chlorophyll-a concentration in turbid productive waters. *Remote Sensing of Environment*, 117, pp. 394–406. https://doi.org/10.1016/j.rse.2011.10.016

Niroumand-Jadidi, M., Bovolo, F., & Bruzzone, L., 2020. Water quality retrieval from Prisma hyperspectral images: First experience in a turbid lake and comparison with sentinel-2. *Remote Sensing*, 12(23), 3984. https://doi.org/10.3390/rs12233984

White, P., Christensen, G. N., Palerud, R., Legovic, T., Rosario, W. R., Lopez, N., Regpala, R. R., Gecek S., & Hernandez, J., 2016. *EMMA (European Union's Emerging Megacities: Mitigation and Adaptation) Project*. EMMA Taal final report [PDF file]. Retrieved from http://aquaculture.asia/files/D8_EMMA_Taal_final_report.pdf